

Separation of uranium anomalies based on geophysical airborne analysis by using Concentration-Area (CA) Fractal Model, Mahneshan 1: 50000 Sheet, NW IRAN

Original

Separation of uranium anomalies based on geophysical airborne analysis by using Concentration-Area (CA) Fractal Model, Mahneshan 1: 50000 Sheet, NW IRAN / Afzal, Peyman; Afshar Zia, Zarifi; Farhadi, Sasan; Wetherelt, Andy; Yasrebi Bijan, Amir. - In: JOURNAL OF MINING AND METALLURGY. SECTION B: METALLURGY. - ISSN 1450-5339. - 48:(2012), pp. 1-11.

Availability:

This version is available at: 11583/2974318 since: 2023-01-03T15:59:13Z

Publisher:

Journal of Mining and Metallurgy, Section B: Metallurgy

Published

DOI:

Terms of use:

This article is made available under terms and conditions as specified in the corresponding bibliographic description in the repository

Publisher copyright

(Article begins on next page)

SEPARATION OF URANIUM ANOMALIES BASED ON GEOPHYSICAL AIRBORNE ANALYSIS BY USING CONCENTRATION-AREA (C-A) FRACTAL MODEL, MAHNESHAN 1:50000 SHEET, NW IRAN

Peyman Afzal^{*,#}, Afshar Zia Zarifi^{**}, Sasan Farhadi Khankandi^{*},
Andy Wetherelt^{***} and Amir Bijan Yasrebi^{***}

^{*}Department of Mining Engineering, South Tehran branch,
Islamic Azad University, Tehran, Iran

^{**}Department of Mining Engineering, Lahijan Branch,
Islamic Azad University, Lahijan, Iran

^{***}Camborne School of Mines, University of Exeter, Penryn, UK

(Received 7 June 2012; Accepted 12 September 2012)

Abstract

The aim of this study is separation of uranium anomalies based on geophysical airborne data by utilizing the Concentration-Area (C-A) fractal model in Mahneshan 1:50000 sheet, NW Iran. Threshold values for the different anomalies of uranium were computed with the statistical method which shows that uranium anomaly commences from 282.1 eppm. Furthermore, the C-A log-log plot of uranium shows existence of two stages of uranium enrichment in this area. The major enrichment for U starts from 331.1 eppm. High intensity anomalies (>562.3 eppm) in the area are located in the central and northern parts of the area. The comparison between achieved results and fault's position patterns shows a positive correlation between uranium anomalies and the faults system in the area. However, mica-schists host high intensive uranium anomalies in the central part of the area. Results analyzed by the C-A fractal model certify that the interpreted anomalies based on the fractal model are accurate in comparison with the chemical analysis of lithogeochemical samples collected from the geophysical airborne anomalies.

Key words: Concentration-Area (C-A) fractal model; Uranium; Airborne geophysical data; Mahneshan; Iran.

1. Introduction

Airborne geophysical data especially radiometric data are used for identification of radioactive anomalies specifically for uranium exploration. Interpretation of this

data is important for mineral exploration specifically radioactive elements [1, 2]. Several methods and models have been used for interpretation of radiometric airborne data [3, 4, 5]. Statistical methods are commonly utilised to identify uranium

[#] Corresponding author: P_Afzal@azad.ac.ir

anomalies and have been applied to the airborne spectrometric data for separation of uranium anomalies from background [1, 6]. In conventional statistical methods, threshold values are considered with respect to mean and standard deviation or median based on a normal or log-normal distribution [7, 8]. Normality or log-normality in statistical methods does not consider the shape, extent and magnitude of anomalous and geological environments which are useful to distinguish geophysical anomalies from the background [9, 10, 11, 12].

In the recent years, models based on fractal geometry as a Non-Euclidean geometry proposed by Mandelbrot (1983) have been widely applied in different branches of geosciences since various geophysical and geochemical populations can be defined by changes in fractal dimensions resulting from analysis of relevant geophysical data [13, 14, 15, 16]. Application of fractal and multifractal models has given rise to a better understanding of geophysical phenomena from micro to macro levels [17, 18, 19]. In addition, fractal dimensions in geological and mineralisation processes correspond to variations in physical attributes such as mineralogy, lithology, stratigraphy, fluid phases, alteration zones and structural feature [20, 21, 22].

The aim of this paper is to use the C-A fractal model to delineate uranium anomalies based on geophysical airborne data, in Mahnesan 1:50000 sheet, NW Iran. In addition, combination and comparison between C-A, geological particulars and lithogeochemical samples to distinguish main anomalies have been carried out.

2. Concentration-area fractal model

The C-A fractal model, which was proposed by Cheng et al. (1994) for division of anomalies and background in geochemical and geophysical exploration, can be addressed as follow:

$$A(\rho \leq v) \propto \rho^{-a1}; A(\rho \geq v) \propto \rho^{-a2} \quad (1)$$

Where $A(\rho \leq v)$ and $A(\rho \geq v)$ illustrate two areas with concentration values less than or equal to and greater than or equal to the contour value ρ ; v indicates the threshold value of an anomaly; and $a1$ and $a2$ are characteristic exponents. Elemental threshold values in this model represent boundaries between different anomalies and background. To calculate $A(\rho \leq v)$ and $A(\rho \geq v)$ in the study, which are the areas enclosed by a contour level ρ in a 2D grid model, the airborne data of ore element concentrations were interpolated by utilization of geostatistical estimation.

3. Geological setting of the Mahnesan 1:50000 sheet

The Mahnesan 1:50000 sheet is situated in the western part of Zanjan province, NW Iran (Fig. 1). The area is located in Uriumia-Dokhtar magmatic belt which hosts many metallic deposits in Iran [8, 23, 24]. There are several metallic prospects and mines especially Angoran Zn and Pb mine named as the biggest Zn-Pb mine in Iran also Cu, Pb, Zn, quarry stones, salt, gypsum and feldspar mines are considerable in the area. Oldest rock types in the area are Pre-Cambrian granites as named Doran granites [25].

There are metamorphic rocks including gneisses, mica-schists, marbles and

amphibolites with high extension in the area. Furthermore, Infra-Cambrian sedimentary units include sandstones, shales and dolomites cover several parts of the area. There are Eocene granitic-granodioritic units in the several parts of

the 1:50000 sheet. Pre-Cambrian green and gray shales and tuffs occur in the central parts of the area (Fig. 1). Moreover, there is a Pre-Cambrian fault zone with a trend of NW-SE [25, 26].

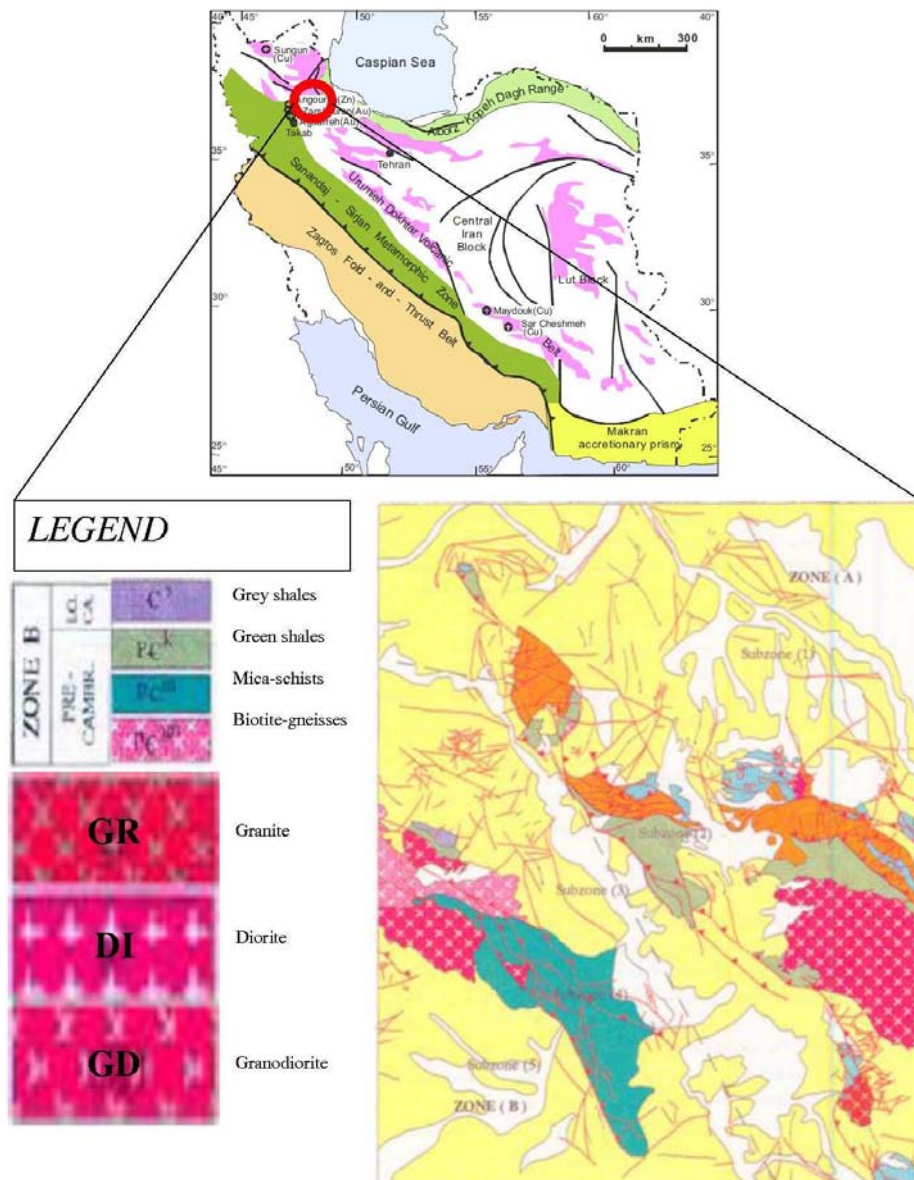


Figure 1. Location the Mahneshan 1:50000 sheet in the structural map of Iran and geological map of Mahneshan 1:50000 sheet [25, 26]

4. Geophysical airborne analysis

55650 radiometric airborne data were collected by Austrex Co. in a grid with $500 \times 300 \text{ m}^2$ cell between air routes surveying during 1976 to 1978. Spacing between flight lines is 300 m with line direction of 41 degree and sample interval of 1 second. Detected parameters of these data include U235, Th232 and K40.

4.1. Statistical analysis

One of the significant methods to separate background from different anomalies is the classical statistics method which can be intended to determine various anomalies if distribution in terms

of geophysical and geochemical data is normal [1, 2, 4, 5, 8, 9].

Uranium histogram for Mahnesan 1:50000 sheet indicates the uranium distribution in the area is normal, as depicted in Fig. 2. According to the normal distribution of the airborne data, different anomalies were identified by using formulas based on mean (M) and standard deviation (SD), as illustrated in table 1. Uranium first threshold value is equal to summation of mean and standard deviation (M+SD) which is 282.1 eppm. Moderate and high intensity anomaly thresholds are equal to $M + 2SD$ (344 eppm) and $M+3SD$ (405.9 eppm), respectively (Table 1).

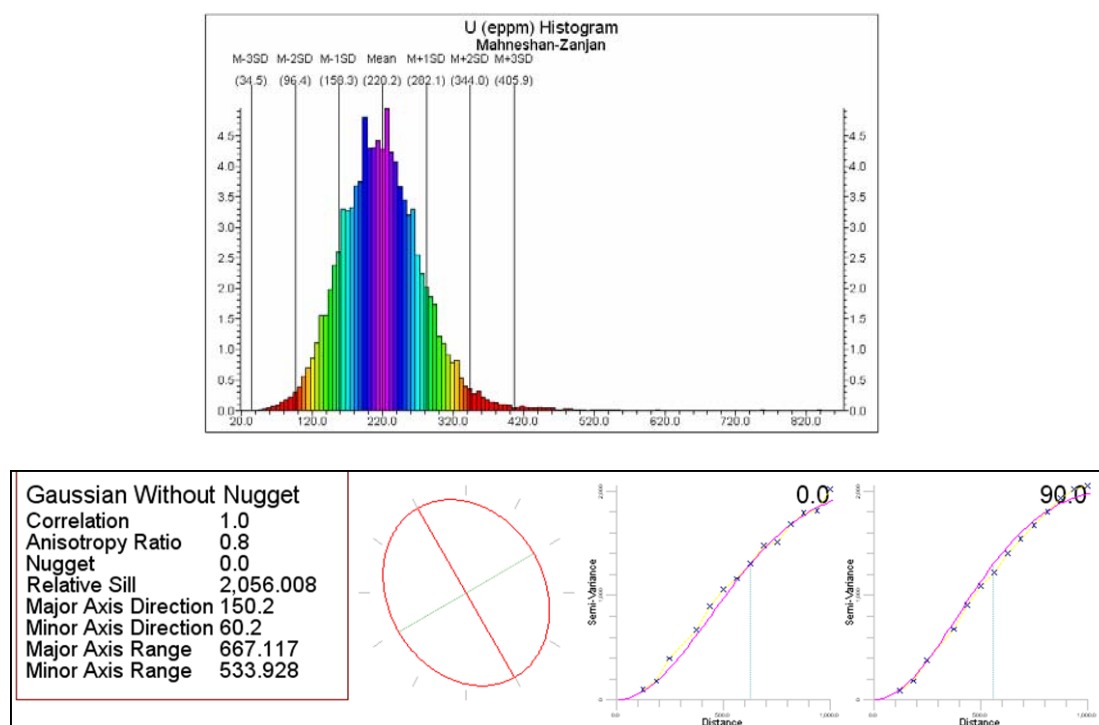


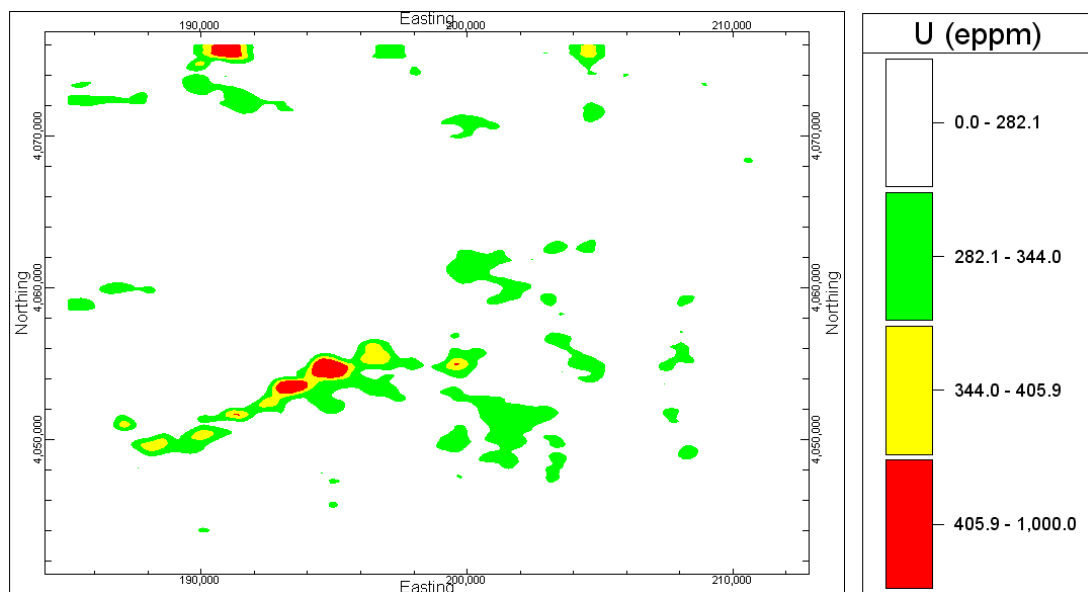
Figure 2. Uranium histogram and variogram in Mahnesan 1:50000 sheet

Table 1. Thresholds of uranium (eppm) in Mahneshan 1:50000 sheet based on classical statistics method

Anomaly Type	U (eppm) threshold	Range of U (eppm)
Low intensity	282.1	282.1-344.0
Moderate intensity	344.0	344.0-405.9
High intensity	405.9	>405.9

Uranium distribution map in the area was generated by RockWorks 15 software in terms of kriging and also uranium was

classified to four populations based on classical statistics method, as illustrated in Fig. 3.

**Figure 3.** Uranium anomalies based on classical statistics in Mahneshan 1:50000 sheet

Ordinary kriging was used because it is compatible with a stationary model; it only involves a variogram, and it is in fact the form of kriging used most [27]. The method estimates values in un-sampled locations based on moving average of the variable of interest satisfying different dispersion forms of data, e.g., sparse sampling points [28]. Ordinary kriging is a spatial estimation method where the error variance is minimized. This error variance is called the kriging variance. It

is based on the configuration of the data and on its variogram also one of the main reasons for utilisation of Kriging is due to the huge amount of samples [29]. As a result of that, there is a good correlation between experimental and standard variograms in this research which represents that the Ordinary Kriging has been intended as the proper estimator (Fig. 2). The studied area was gridded to 75×75 m² cells for evaluation of uranium distribution in the sheet. Anomalous parts

of uranium in the area are located in the small parts of northern, southern and specifically in the central parts of this sheet. High intensity anomalies occur in small parts of the northern and central areas of the sheet (Fig. 3).

4.2. C-A model

C-A log-log plot of uranium was created in Mahneshan 1:50000 sheet. Uranium populations were separated by fitted linear segments and breakpoints in

the log-log plot (Fig. 4). Uranium distribution in the area depicts a multifractal model in regard to its log-log plot. As a result, two phases for uranium mineralization are present in the Mahneshan area. Uranium threshold values are 199.5, 331.1 and 562.3 eppm which are low, moderate and high intensity anomaly threshold values respectively, as illustrated in table 2.

Distribution map of uranium and fault's positions in the area were constructed by RockWorks 15 (Fig. 5).

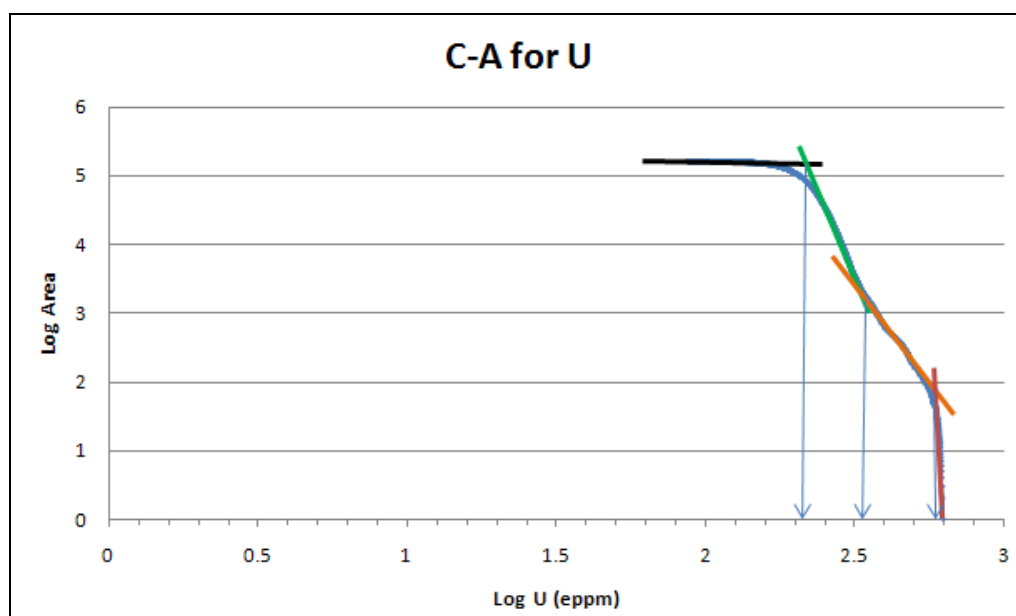


Figure 4. C-A log-log graph for uranium in Mahneshan area

Table 2. Thresholds of uranium (eppm) in Mahneshan 1:50000 sheet based on concentration-area (C-A) model

Anomaly Type	U (eppm) threshold	Range of U (eppm)
Low intensity	199.5	199.5-331.1
Moderate intensity	331.1	331.1-562.3
High intensity	562.3	>562.3

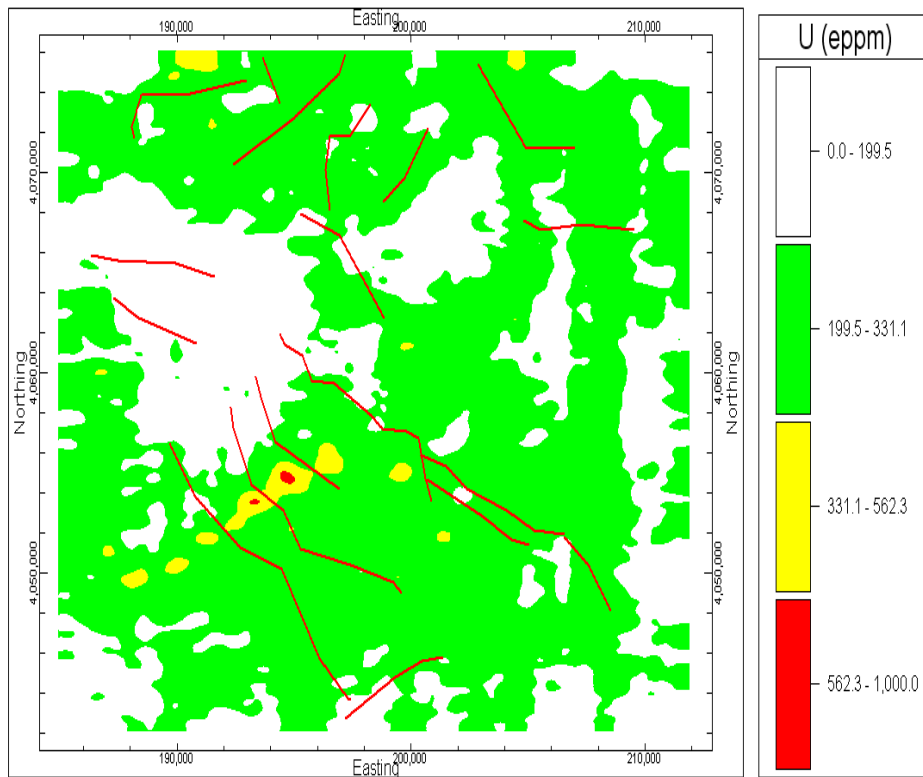


Figure 5. Uranium anomalies' distribution map based on C-A method imposed on fault location maps (red lines)

Uranium high intensity anomalies, higher than 562.3 eppm, are located in the central parts of Mahneshan 1:50000 sheet and moderate intensity anomalies, between 331.1 and 562.3 eppm, occur in the central, north and SW parts of this area.

5. Correlation between C-A model and geological particulars

Thresholds results from C-A model are correlated to geological particulars consisting of lithological units and faults. Faults and U anomalies have a positive relationship in Mahneshan 1:50000 sheet representing that the U main enrichment

has been made in the intersections of faults therefore, high grade uranium anomalies (>562.3 eppm) are present inside and within the fault zones (Fig. 5).

Comparison between rock types and uranium anomalies illustrates that the main anomalous parts (>331.1 eppm) correspond with mica-schists, as depicted in Fig. 6. Magmatic rocks consisting of granodiorite and granites associated with low intensity anomalies are in the western, eastern and SE parts of the area, as illustrated in Fig. 6. Moreover, shales including low intensive uranium anomalies are in the eastern part of the area (Fig. 6).

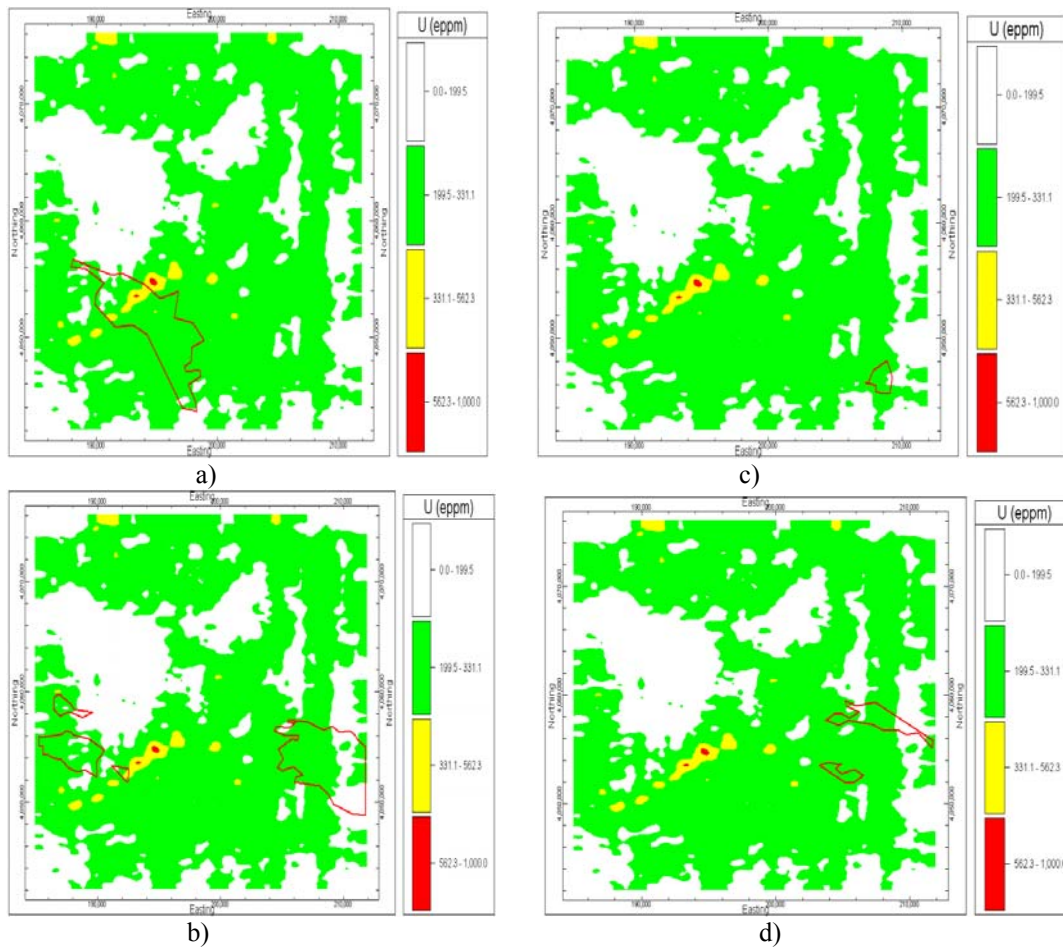


Figure 6. Correlation between uranium anomalies and rock types (red polygons) consist of a) mica-schist's position, b) granodiorites, c) granite and d) situation of shales

6. Control anomalies with litho-chemical samples

Three lithogeochemical samples were collected from uranium anomalies consisting of M1 from mica-schist, M2 from granodiorite and M3 from granite (Fig. 7) and analyzed by ICP-MS method. M1 was collected from high intensive uranium anomaly (>562.3 eppm) and its

uranium equal to 11.5 ppm. M2 associated with moderate intensity anomaly (331.1-562.3 eppm) has 7.2 ppm uranium concentration. M3 was collected from low intensive anomaly (<199.5 eppm) and its uranium value is 5.3 ppm. The uranium concentrations of the samples have proper correlation with geophysical airborne anomalies resulted by C-A method.

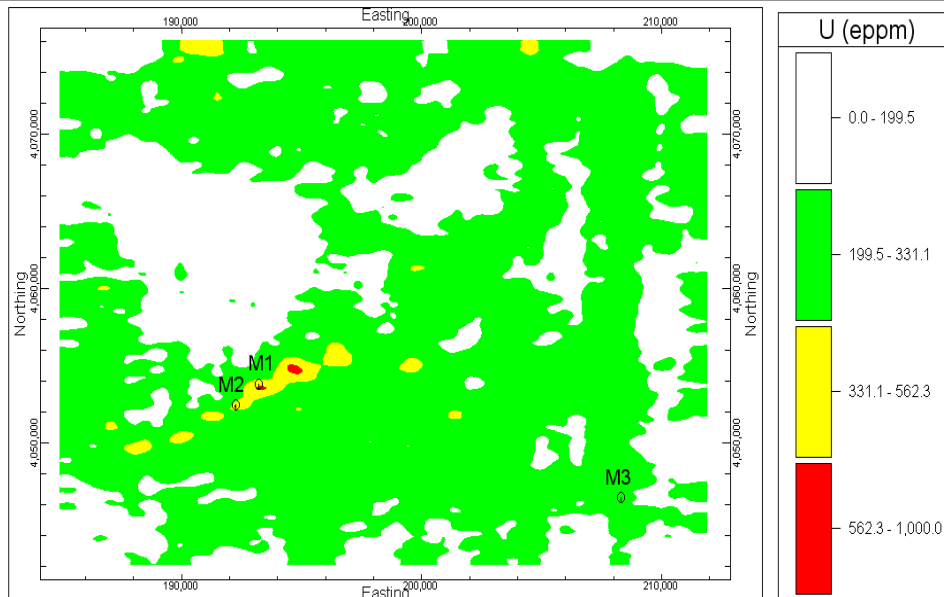


Figure 7. Collected lithogeochemical samples from uranium anomalies

6. Conclusion

Results obtained by study on Mahneshan 1:50000 sheet indicate the potential use of the C-A model for radiometric airborne anomaly separation as an appropriate tool for geophysical exploration. Log-log plot for uranium in the area shows a multifractal model and two phases for uranium enrichment in the sheet. Uranium anomalies resulted from C-A model and statistical method outline that main uranium anomalies are located in the central parts of the area. Resulted uranium anomalies in the area based on classical statistics are similar to anomalies from C-A model because uranium distribution is normal in this area. According to correlation between geological particulars and uranium anomalies achieved by C-A model, mica-schists were associated with the high and moderately anomalies of uranium in Mahneshan 1:50000 sheet. There is a

proper correlation between the calculated anomalies and the position of faults in the area since the main uranium anomalies (> 331.1 eppm) were located inside of faults. Results of three analyzed samples by ICP-MS method show that uranium concentrations have a positive correlation with anomalies derived via C-A model.

7. Acknowledgement

The paper was extracted from a research project entitled “Geophysical airborne data by using classical statistics and fractal methods in Mahneshan 1:50000 sheet” by supporting of Islamic Azad University, South Tehran branch. The authors wish to acknowledge the research deputy of Islamic Azad University, South Tehran branch for financial support of this study. The authors would like to thank the editors and reviewers of this paper for their comments and valuable remarks.

8. References

- [1] S.H. Abd El Nabi, Statistical evaluation of airborne gamma ray spectrometric data from the Magal Gebriel area, south Eastern Desert, Egypt, *Journal of Applied Geophysics*, 34 (1) (1995), 47-54.
- [2] H. Ranjbar, H. Hassanzadeh, M. Torabi, O. Ilaghi, Integration and analysis of airborne geophysical data of the Darrehzar area, Kerman Province, Iran, using principal component analysis, *Journal of Applied Geophysics*, 48 (1) (2001), 33-41.
- [3] M.L. Airo, S. Mertanen, Magnetic signatures related to orogenic gold mineralization, Central Lapland Greenstone Belt, Finland, *Journal of Applied Geophysics*, 64 (1-2) (2008), 14-24.
- [4] S.H. Abd El Nabi, Role of γ -ray spectrometry in detecting potassic alteration associated with Um Ba'anib granitic gneiss and metasediments, G. Meatiq area, Central Eastern Desert, Egypt, *Arabian Journal of Geosciences*, doi 10.1007/s12517-011-0378-4, (2011).
- [5] S. Gaci, N. Zaourar, L. Briquieu, M. Djeddi, Impact of the pre-processings on the fractal properties of the airborne gamma ray measurements: a case study from Hoggar (Algeria), *Arabian Journal of Geosciences*, doi 10.1007/s12517-011-0407-3, (2011).
- [6] J. Asfahani, R. Al-Hent, M. Aissa, Uranium statistical and geological evaluation of airborne spectrometric data in the Al-Awabed region and its surroundings (Area-3), Northern Palmyrides, Syria, *Applied Radiation and Isotopes*, 67 (4) (2009), 654-663.
- [7] M.A. El-Sadek, A. Ammar, M.A. Omran, H.M. Abu Elkheer, Airborne γ -ray spectrometric characteristics of lithological units and environmental issues in the Bahariya Oases area in the northern part of western desert, Egypt, *Arabian Journal of Geosciences*, 4 (7-8) (2011), 1151-1161.
- [8] P. Afzal, A. Khakzad, P. Moarefvand, N. Rashidnejad Omran, B. Esfandiari, Y. Fadakar Alghalandis, Geochemical anomaly separation by multifractal modeling in Kahang (Gor Gor) porphyry system, Central Iran, *Journal of Geochemical Exploration*, 104 (2010), 34-46.
- [9] J.C. Davis, *Statistics and data analysis in Geology* (3th ed.), John Wiley & Sons Inc., New York, 2002.
- [10] C. Reimann, P. Filzmoser, R.G. Garrett, Background and threshold: critical comparison of methods of determination, *Science of The Total Environment*, 346 (2005), 1-16.
- [11] D.L. Turcotte, Fractals in geology and geophysics, *Pure and applied Geophysics*, 131 (1) (1989), 171-196.
- [12] D.L. Turcotte, *Fractals and chaos in geology and geophysics*, Cambridge University Press, Cambridge, 1997, p. 398.
- [13] D.L. Turcotte, The relationship of fractals in geophysics to "the new

-
- science”, *Chaos, Solitons & Fractals*, 19 (2) (2004), 255-258.
- [14] C.C. Barton, P.R. La Pointe, *Fractals in the earth sciences*, Plenum Press, New York, 1995, p. 265.
- [15] B. Bolviken, P.R. Stokke, J. Feder, T. Jossang, The fractal nature of geochemical landscapes, *Journal of Geochemical exploration* 43 (1992), 91-109.
- [16] C. Scholz, B.B. Mandelbrot, Special issue on fractals in geology and geophysics, *Pure and applied Geophysics*, 131 (1992), 96-171.
- [17] W. Shen, C. Fang, D. Zhang, Fractal and chaos research of geo-magnetic polarity reversal, *Earth Science Frontiers*, 16 (5) (2009), 201-206.
- [18] M. Hashemi, P. Afzal, I. Rasa, M. Noghreian, Kh. Khosro Tehrani, M. Vosoughi Abedini, Geochemical anomaly separation by concentration - area fractal model in Bardaskan area, NE Iran, *Journal of Mining and Metallurgy Section A: Mining*, 46 (1) (2010), 1 - 10.
- [19] Q. Cheng, F.P. Agterberg, S.B. Ballantyne, The separation of geochemical anomalies from background by fractal methods, *Journal of Geochemical Exploration*, 51 (1994), 109-130.
- [20] N. Rashidnejad Omran, P. Afzal, H. Harati, P. Moarefvand, H. Asadi Haroni, L. Daneshvar Saein, Application of power-law frequency fractal model in determination of vertical geochemical distribution of Cu in Kahang porphyry deposit, Central Iran, *Journal of Mining and Metallurgy Section A: Mining*, 47 (1) (2011), 1 - 8.
- [21] V.P. Dimri, *Fractal behavior of the Earth System*, Springer, Berlin, 2005, p. 208.
- [22] B.B. Mandelbrot, *The fractal geometry of nature*, Freeman, San Francisco, 1983, p. 468.
- [23] M. Alavi, Tectonic of Zagros orogenic belt of Iran: new data and interpretations, *Tectonophysics*, 229 (1994), 211-238.
- [24] M. Berberian, G.C. King, Towards a paleogeography and tectonic evolution of Iran, *Canadian Journal of Earth Sciences*, 18 (1981), 210-265.
- [25] M. Kiani, Geological map of Iran 1:100000 sheet No. 5563. Geological survey of Iran, 2001.
- [26] F. Daliran, The carbonate rock-hosted epithermal gold deposit of Agdarreh, Takab geothermal field, NW Iran - hydrothermal alteration and mineralization, *Mineralium Deposita*, 43 (2008), 383-404.
- [27] J.P. Chilès, P. Delfiner, *Geostatistics: Modeling Spatial Uncertainty*, Wiley, New York, 1999, p. 695.
- [28] P. Goovaerts, *Geostatistics for natural resources evaluation*, Oxford University Press, New York, 1997, p. 496.
- [29] J.K. Yamamoto, Comparing ordinary kriging interpolation variance and indicator kriging conditional variance for assessing uncertainties at unsampled locations, In: S. Dessureault, R. Ganguli, V.J. Kecojevic, J.G. Dwyer, (Eds.), *Application of computers and operations research in the mineral industry*, Balkema, 2005.